Chapter 4

Investigation of components of mTORC1 and mTORC2 complexes in severely insulin resistant patients

4.1 Summary

Components of the mammalian target of rapamycin (mTOR) pathway are key players in insulin signalling. mTOR exists in two distinct complexes: mTORC1, which contains mTOR, Raptor, and GβL, and mTORC2, which contains mTOR, Rictor, GβL, and MAPKAP1. Hyperactivation of mTORC1 and its downstream effectors is associated with serine phosphorylation of insulin receptor substrates and inhibition of insulin signalling. mTORC2 is required for insulin-stimulated phosphorylation of AKT, which goes on to repress AS160 to promote GLUT4-mediated glucose uptake. The aim of this study was to screen members of the mTOR pathway in human syndromes of insulin resistance for potentially pathogenic mutations. I sequenced exons, exon-intron boundaries and 3'UTR of *mTOR*, *Raptor*, *Rictor*, *GβL*, *MAPKAP1*, and *AS160* in 158 patients with syndromes of severe insulin resistance, as well as 11 Indian and 48 European controls. I detected 12 rare non-synonymous variants across all genes, 11 of which were considered unlikely to be pathogenic in a fully penetrant manner. However, a nonsense mutation in *AS160*, R636X, co-segregated with high peak-to-fasting insulin levels in a family with five affected individuals. The truncated protein significantly reduced insulin-stimulated GLUT4 translocation to the cell surface *in vitro* and was able to bind full length AS160, providing a possible mechanism for a dominant negative effect. These studies suggest that mutations in genes encoding components of mTOR complexes are not common causes of severe insulin resistance, whereas a stop mutation in *AS160* causes an inherited defect in insulin-stimulated glucose transporter translocation (Satya et al., manuscript submitted).

4.2 Introduction

4.2.1 The mammalian target of rapamycin

The mammalian target of rapamycin (mTOR) (also known as FKBP-rapamycin associated protein (FRAP1), rapamycin and FKBP target (RAFT), and rapamycin target (RAPT)) is an evolutionarily conserved large serine/threonine protein kinase belonging to the phosphatitidylinositol kinase-related kinase (PIKK) family (Abraham 2004). It is a central component of a complex signalling network that regulates cell growth and development in response to nutritional, hormonal, energy- and stress-related cues (Sarbassov et al. 2005a; Wullschleger et al. 2006). TOR genes were first identified in yeast during a screen for mutations conferring resistance to the growth inhibitor, rapamycin (Heitman et al. 1991). A complex of rapamycin and cofactor, FKBP12, bind mTOR at its FKBP-rapamycin binding (FRB) domain and inhibit its kinase activity.

4.2.2 mTOR complexes

mTOR exists in at least two distinct complexes, mammalian target of rapamycin complex 1 (mTORC1) and 2 (mTORC2), both of which play roles in insulin signalling (Figure 4.1). In mTORC1, mTOR is accompanied by the regulatory associated protein of TOR (Raptor) and GβL (also known as mLST8), both of which are required for mTORC1 signalling. The mTORC2 complex comprises mTOR, rapamycin-insensitive companion of TOR (Rictor), GßL, and mitogen-activated protein kinase-associated protein 1 (MAPKAP1 (also known as SIN1)). Rictor is a large protein with no obvious catalytic motifs and MAPKAP1 is a member of the poorly conserved stress kinase-interacting protein 1 (SIN1) family. Both are essential for mTORC2 assembly and function. Though this complex is resistant to acute exposure to rapamycin, long-term administration can block its assembly. This probably occurs as a result of decreased availability of free mTOR to bind components of mTORC2 (Barilli et al. 2008; Frias et al. 2006; Sarbassov et al. 2006; Varma et al. 2008).

4.2.3 The role of mTORC1 in insulin signaling

As decribed in Chapter 1, mTORC1 is an important mediator of insulin and nutrient-stimulated protein synthesis and cell growth (Figure 4.1). Another critical kinase within the insulin signalling pathway, AKT, indirectly activates mTORC1 by inhibiting the tuberous sclerosis protein complex (TSC1-TSC2) (reviewed in (Wullschleger et al. 2006)). TSC1-TSC2 negatively regulates mTORC1 by acting as a guanine triphosphatase (GTPase) activating protein (GAP) for Ras homolog enriched in brain (Rheb), which is able to activate mTORC1 activity in its GTP-bound form (Manning and Cantley 2003; Tee et al. 2003). mTORC1 is then able to activate mRNA translation through phosphorylation of p70 ribosomal S6 kinase (S6K1) and the eukaryotic translation initiation factor (eIF4E)-binding protein (4E-BP1). Recent studies have shown that activation of the mTORC1/S6K1 pathway is involved in a negative feedback mechanism that inhibits insulin signal transduction (Haruta et al. 2000; Tremblay and Marette 2001).

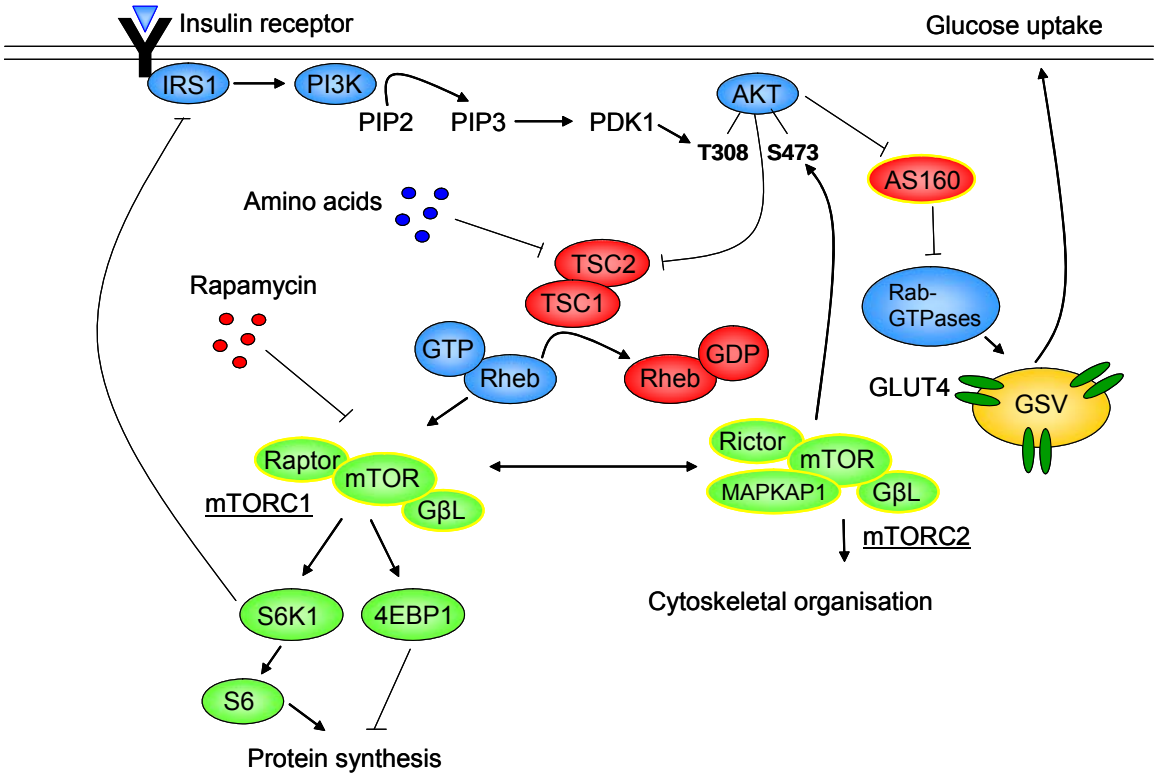

Figure 4.1 Insulin signalling through mTORC1 and mTORC2
Insulin binding to the insulin receptor in target cells triggers a signalling cascade leading to activation of AKT. Full activity of AKT requires phosphorylation by PDK1 on T308 and by mTORC2 on S473. AKT mediates insulin-induced stimulation of mTORC1 activity and protein synthesis, and prevents inhibition of glucose uptake by AS160. mTORC1 substrate S6K1 participates in a negative feedback loop to attenuate further insulin signalling. GSV = GLUT4 storage vesicle.

4.2.4 mTORC1/S6K1 pathway augments serine phosphorylation of IRS proteins

Serine phosphorylation of IRS proteins has emerged as a key event underlying the induction of insulin resistance (Zick 2001). There are several mechanisms by which serine phosphorylation inhibits IRS protein activity, including inducing release of IRS proteins from intracellular complexes that hold them in close proximity to the insulin receptor (Heller-Harrison et al. 1995), and inducing their degradation (Pederson et al. 2001). Activation of the mTORC1/S6K1 pathway by insulin or amino acids has been shown to augment serine phosphorylation on IRS1 and thereby suppress insulin signalling in myocytes and adipocytes (Haruta et al. 2000; Takano et al. 2001; Tremblay et al. 2005; Tremblay and Marette 2001). These effects were blocked by rapamycin treatment. Constitutively active mTORC1/S6K1 as a result of disruption of

TSC1/TSC2, or ectopic expression of Rheb, also caused phosphorylation and downregulation of insulin receptor substrates and insulin resistance *in vitro* (Harrington et al. 2004; Shah et al. 2004).

Both mTOR and S6K1 have been shown to directly catalyse serine phosphorylation of IRS1 *in vitro* (Harrington et al. 2004; Ozes et al. 2001). Conversely, siRNA-mediated knockdown of S6K1 decreased IRS1 serine phosphorylation and increased insulin-induced AKT phosphorylation (Khamzina et al. 2005; Um et al. 2004) and mice deficient for S6K1 or resistant to phosphorylation of its substrate, the 40S ribosomal protein S6, exhibited greater insulin sensitivity (Pende et al. 2000; Ruvinsky et al. 2005; Um et al. 2004). These mice were also glucose intolerant due to reduced pancreatic beta-cell size and consequent hypoinsulinaemia, indicating a role for S6K1 in pancreatic beta-cell growth.

4.2.5 mTORC1/S6K1 provides a mechanism for diet-induced insulin resistance

Given the nutrient-sensing role of the mTORC1/S6K1 it is plausible that enhanced stimulation of this pathway might cause insulin resistance under physiological conditions of over-nutrition, such as obesity. Indeed, enhanced mTOR/S6K1 activation, IRS1 serine phosphorylation, and reduced AKT activation have been observed in wild-type mice fed on a high fat diet and in rodent models of obesity (Khamzina et al. 2005; Um et al. 2004). In contrast, S6K1-deficient mice are also protected against diet-induced obesity and insulin resistance (Um et al. 2004). Furthermore, in humans, mTOR/S6K1 activation by amino acid infusion causes IRS1 serine phosphorylation and insulin resistance in a rapamycin-sensitive manner (Krebs et al. 2007; Tremblay et al. 2005).

4.2.6 mTORC1/S6K1 signaling and β-cell function

IRS2, the most abundant and functionally important member of the IRS family in pancreatic beta-cells, is also down-regulated by mTOR/S6K1 signaling (Briaud et al. 2005; Shah et al. 2004). Chronic exposure of pancreatic beta-cells to glucose or

IGF1 increased serine/threonine phosphorylation and proteasomal degradation of IRS2 leading to insulin resistance and apoptosis (Briaud et al. 2005). These effects were blocked by rapamycin suggesting that inhibition of mTORC1/S6K1 might alleviate insulin resistance and improve β-cell survival under conditions of chronic hyperglycaemia. However, long-term rapamycin treatment actually increased insulin resistance in kidney transplanted patients (Di Paolo et al. 2006) and in diabetic *P. Obesus* Israeli sand rats (Fraenkel et al. 2008). The latter also experienced a reduction in beta-cell survival and glucose-stimulated insulin secretion and biosynthesis, which interfered with compensatory insulin secretion to overcome insulin resistance and consequently worsened hyperglycaemia. The discrepancy between the effects of rapamycin in these and previous studies could reflect the difference in metabolic backgrounds of subjects, and the duration of rapamycin treatment. Interestingly, there is evidence to suggest that long-term rapamycin administration inhibits the function of the mTORC2 complex which, as described next, also plays a role in insulin signaling.

4.2.7 mTORC2 plays a role in cytoskeletal organisation and AKT phosphorylation

mTORC2 plays a critical role in organisation of the actin cytoskeleton (Jacinto et al. 2004; Sarbassov et al. 2004) and phosphorylation of AKT Ser473 (Ali and Sabatini 2005; Hresko and Mueckler 2005; Sarbassov et al. 2005b). Rictor-, GßL-, and MAPKAP1-deficient mouse embryos die at midgestation, most likely as a result of defective fetal vascular development (Guertin et al. 2006; Jacinto et al. 2006; Shiota et al. 2006). Furthermore, basal and insulin-stimulated AKT Ser473 phosphorylation is impaired in Rictor-, GßL-, and MAPKAP-deficient mouse embryonic fibroblasts (MEFs) (Guertin et al. 2006; Jacinto et al. 2006), Drosophila, and mammalian cells (Frias et al. 2006; Yang et al. 2006). AKT phosphorylation of Thr308 is also impaired suggesting that mTORC2 facilitates this phosphorylation.

4.2.8 mTORC2 plays a role in insulin-stimulated glucose uptake

Muscle-specific *Rictor* knock-out mice displayed decreased insulin-stimulated AKT Ser473 phosphorylation and, additionally, impaired insulin-stimulated glucose uptake (Kumar et al. 2008). Impaired insulin-stimulated glucose uptake could be mediated by disrupted downstream signalling of AKT, which regulates GLUT4 redistribution from intracellular sites to the cell surface in muscle and fat tissues. Indeed, Rictor-deficient muscles show diminished phosphorylation of AKT substrate of 160 kDa (AS160, also known as TBC1D4) (Kane et al. 2002), which is phosphorylated on several residues in response to insulin in a PI3K-dependent manner (Bruss et al. 2005; Sano et al. 2003). AS160 contains two phosphotyrosine binding domains and a C-terminal Rab-GAP domain, which is proposed to promote hydrolysis of Rab proteins on the GLUT4 storage vesicle (GSV). Insulin-stimulated AS160 phosphorylation inactivates its Rab-GAP activity allowing GTP-bound GSV-associated Rabs to promote processes that lead to GLUT4 translocation to the plasma membrane. In support of this, expression of phosphorylation-resistant forms of AS160 reduces insulin-stimulated GLUT4 translocation to the cell surface (Kramer et al. 2006; Sano et al. 2003; Thong et al. 2007), and RNAi-mediated knockdown of AS160 increases basal GLUT4 levels at the cell surface (Eguez et al. 2005; Larance et al. 2005) in adipocytes.

4.2.9 Genetic studies

Mutations in the insulin receptor signalling pathway can lead to syndromes of insulin resistance (George et al. 2004; Krook and O'Rahilly 1996), therefore it is reasonable to postulate that other genes downstream of the INSR may also be involved in these syndromes. Indeed variants in genes encoding downstream components of the insulin signalling cascade have been detected by our group (in collaboration with Steven O'Rahilly) in syndromes of insulin resistance, for example, *IRS1* (Berger et al. 2002), *IRS2* (Bottomley, submitted), *AKT2* (George et al. 2004; Tan et al. 2007),

GLUT4 (unpublished), and some of these variants have been shown to be causal of disease (George et al. 2004). However, to my knowledge, there have been no efforts to screen components of mTOR complexes or *AS160* for mutations involved in insulin resistant diseases. As mTORC1 is involved in a negative feedback loop that blunts insulin signalling by inhibition of IRS1 and IRS2, and as mTORC2 is one of two known kinases that target AKT, which phosphorylates AS160 to promote insulin-stimulated glucose uptake in muscle and fat, I selected genes encoding components of mTORC1 and mTORC2 complexes and AS160 as candidates for syndromes of insulin resistance.

4.2.10 Aims of this study

To sequence genes encoding components of mTORC1 and mTORC2, and AS160, in 158 patients with syndromes of severe insulin resistance to look for potentially pathogenic mutations.

4.3 Results

4.3.1 *mTOR* sequencing in the SIR cohort

A total of 129 variants were detected in *mTOR* in insulin resistant patients (Appendix Table A9), 17 of which were present in the coding sequence (Table 4.1 and Figure 4.2). Coding sequence variants that did not alter the amino acid sequence (shown below the schematic in Figure 4.2) and/or that were also present in controls were considered unlikely to be pathogenic. This left only one rare nonsynonymous variant, V455L, after reconfirmation in genomic DNA had been carried out (underlined above the schematic in Figure 4.2).

4.3.2.1 Investigation of the V455L variation

V455L is present in heterozygous form in an Iranian female with hyperandrogenism, insulin resistance and acanthosis nigricans, and absent from 48 Iranian controls on the HGDP panel. No family members were available for co-segregation analysis so I assessed the likelihood that the variant was pathogenic by its evolutionary conservation and predicted functional effect according to various bioinformatics programs. The valine residue at position 455 is conserved in chimpanzee, mouse, rat, chicken, and opossum but not zebrafish, fruit fly, or either TOR1 or TOR2 in budding yeast (Figure 4.3). The V455L change is predicted to be benign by web-based programs SIFT, PolyPhen and PANTHER. Given this data and the chemical similarity between valine and leucine, I decided not to pursue this variant further.

Table 4.1 *mTOR* coding sequence variants detected in a cohort of severe insulin resistant patients and 11 Indian and 23 CEPH controls

Genic position	Genomic position	Minor|Major allele	Protein consequence	MAF in SIR	Detected in controls?	rs ID
Exon 7	11230691	T|C	H296H	0.006		
Exon 9	**11225807**	**C|G**	**V455L**	**0.004**	**No**	
Exon 10	11224301	C|T	D479D	0.301		rs1135172
Exon 15	11216130	G|C	A778G	0.003	Yes	
Exon 15	11216051	G|A	E804E	0.003		
Exon 19	11211537	A|G	L935L	0.004		
Exon 19	11211345	C|T	N999N	0.253		rs1064261
Exon 23	11195055	C|G	R1154R	0.05		rs17036536
Exon 24	11193482	C|T	D1210D	0.005		
Exon 33	11127645	G|A	A1577A	0.004		rs1057079
Exon 39	11113317	T|C	A1832A	0.044		rs17848553
Exon 39	11113233	T|C	S1851S	0.281		rs2275527
Exon 43	11110729	A|G	T1984T	0.006		
Exon 47	11107180	C|T	L2208L	0.007		
Exon 48	11104650	T|C	L2261L	0.003		
Exon 49	11103914	G|A	L2303L	0.1735		rs1112169
Exon 56	11092007	T|C	D2485D	0.01		

Genomic coordinates correspond to NCBI Build 36.

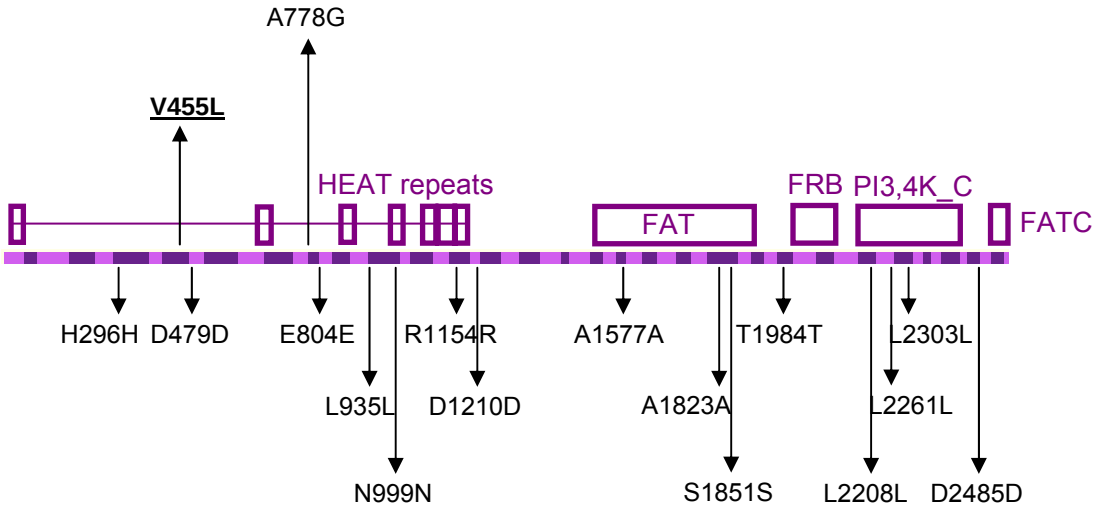

Figure 4.2 Coding *mTOR* variants in the SIR cohort
Schematic of the mTOR protein showing exons in alternating bright and dark purple and known functional domains in boxes. Arrows indicate the location of coding SNPs detected in *mTOR* by sequencing 158 patients with syndromes of severe insulin resistance. Non-synonymous variants are above the schematic and synonymous variants are below the schematic. Non-synonymous mutations absent from control samples were considered potentially pathogenic (underlined). FAT (amino acids 1513-1910) = FRAP-ATM-TRAPP domain, FRB (amino acids 2015-2114) = FKBP12-rapamycin binding, PI3,4K_C (amino acids 2181-2431) = PI3,4-kinase, catalytic domain, and FATC (amino acids 2517-2549) = FAT C-terminus domain.

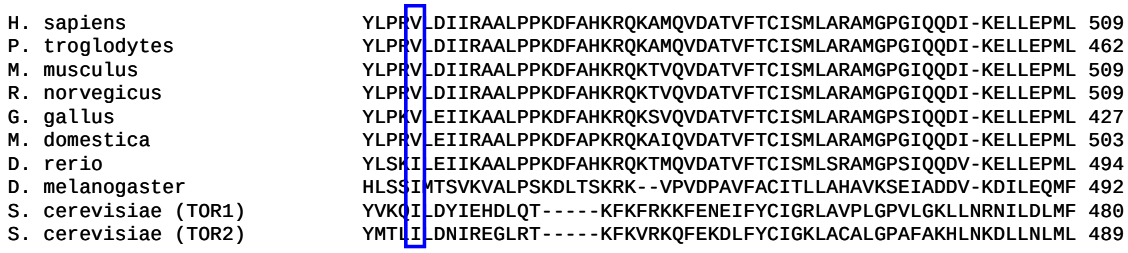

Figure 4.3 Multiple sequence alignments (using ClustalW) of *mTOR* V455 and flanking protein sequence.

4.3.2 *Rictor* sequencing in the SIR cohort

A total of 88 variants were detected in insulin resistant patients (Table A10), 10 of which were present in the coding sequence (Table 4.2 and Figure 4.4). Coding sequence variants that did not alter the amino acid sequence (shown below the schematic in Figure 4.4) and/or that were also present in controls were considered unlikely to be pathogenic. This left a homozygous non-synonymous variation, A3V.

4.3.2.1 Investigation of the A3V variation

A3V was detected in an Asian female with acanthosis nigricans and severe insulin resistance whose parents were first cousins. The variant was not present in 32 Indian samples and 28 European samples from the CIN panel. Family DNA was not available for co-segregation analysis but as alanine and valine residues have similar biochemical properties, the variant is predicted benign by PolyPhen and is not present in a conserved portion of the peptide sequence (Figure 4.5). I did not prioritise it for further analysis.

Table 4.2 *Rictor* coding sequence variants detected in a cohort of severe insulin resistant patients and 11 Indian and 23 CEPH controls

Genic position	Genomic position	Minor|Major allele	Protein consequence	MAF in SIR	Detected in controls?	rs ID
Exon 1	39110229	A|G	A3V	0.0054	No	
Exon 5	39038462	G|A	R108R	0.003		
Exon 17	38998810	C|T	I497I	0.003		
Exon 23	38994634	G|A	E745E	0.007		
Exon 23	38994622	C|T	N749N	0.007		
Exon 25	38993577	A|T	I811I	0.003		
Exon 26	38991553	T|C	S837F	0.299	Yes	rs2043112
Exon 31	38986533	C|T	S1058S	0.033		rs2115949
Exon 31	38986023	T|C	G1228G	0.003		
Exon 33	38982400	C|T	I1442I	0.002		
Exon 38	38978206	T|C	T1695I	0.017	Yes	

Genomic coordinates correspond to NCBI Build 36.

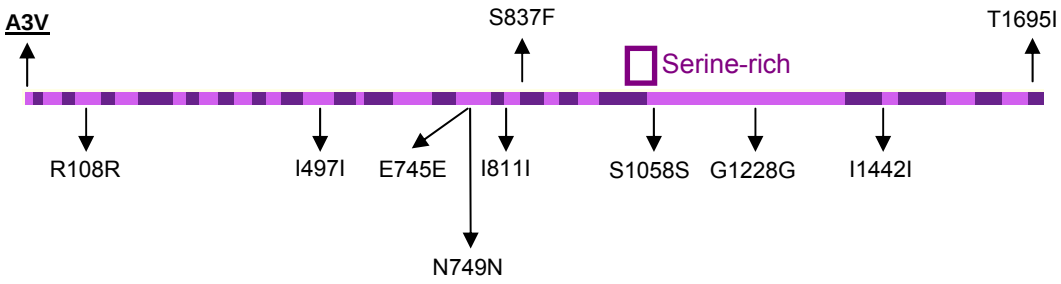

Figure 4.4 Coding *Rictor* variants in the SIR cohort
Schematic of the Rictor protein showing exons in alternating bright and dark purple and features of the peptide sequence in boxes. Arrows indicate the location of coding SNPs detected in *Rictor* by sequencing 158 patients with syndromes of severe insulin resistance. Non-synonymous variants are above the schematic and synonymous variants are below the schematic. One of the non-synonymous variants (above the schematic) was absent from controls and was therefore considered potentially pathogenic.

```
H. sapiens          -----MAAIGRGRSLKNLRVRGRND--SGEENVPLDLTREPSDNLREILQNVARLQGVSN
P. troglodytes      -----MAAIGRGRSLKNLRVRGRND--SGEENVPLDLTREPSDNLREILQNVARLQGVSN
M. musculus         -----MAAIGRGRSLKNLRIRGRND--SGEENVPLDLTREPSDNLREILQNVAKLQGVSN
R. norvegicus       ----------------------------------------EPSDNLREILQNVAKLQGVSN
M. domesticus       -----MAASVRGRSLKHLRIRGRND--SGEENVPLDLTREPYDNLREILQNVAKLQGVSN
G. gallus           -----LTLFGEGEKIESCEYRGNNNKAVQEDDLHLQLGAEPCDNMREILQNVAKLQGVSN
D. melanogaster     MASQHSSWRFGKRSKLQLRIKVSQD---PEDFYRLDPQRSAAENAFEIYS-MLCLEETRD
S. cerevisiae       ----------------MSIPHSAK-----QSSPLSSRRRSVTNTTPLLTPRHSRDNSS-
```

Figure 4.5 Multiple sequence alignment (using ClustalW) around *Rictor* A3 residue

4.3.3 *GβL* sequencing in the SIR cohort

Only ten variants were detected in insulin resistant patients (Appendix Table A11) as a result of *GβL* sequencing, 4 of which were present in the coding sequence (Table 4.3 and Figure 4.6). Two of the variants altered the amino acid sequence of the protein, A88V and E299D (underlined in Figure 4.6), and were absent from 47 Indian and 47 European controls on the CIN panel and a further 48 CEPH controls.

4.3.3.1 Investigation of the A88V variation

A88 is conserved in chimpanzee, mouse and rat but not opossum or any of the non-mammalian organisms investigated (Figure 4.7). A change from alanine to valine was detected as heterozygous in the same white, European male that carried the *LPIN1* G582R variant (see Chapter 3.3.2 for details). Briefly, this patient has a complex syndrome including severe insulin resistance and peripheral neuropathy. As DNA from first-degree relatives was available I sequenced family members for co-segregation analysis (Figure 4.8). The father (who has diabetes) and two unaffected sisters also carry the A88V variant so this change is unlikely to be causing disease in the patient. Furthermore, co-segregation analysis does not support an interaction between *LPIN1* G582R and *GβL* A88V resulting in disease as the father also carries both variants and does not share the features of the complex syndrome exhibited by the proband.

Table 4.3 *GβL* coding sequence variants detected in a cohort of severe insulin resistant patients and 11 Indian and 23 CEPH controls

Genic position	Genomic position	Minor|Major allele	Protein consequence	MAF in SIR	Detected in controls?	rs ID
Exon 4	2196583	T|C	A88V	0.006	No	
Exon 5	2197106	C|G	P137P	0.372		rs26862
Exon 9	2198768	A|G	S289S	0.007		rs11863256
Exon 9	2198798	C|G	E299D	0.006	No	

Genomic coordinates correspond to NCBI Build 36.

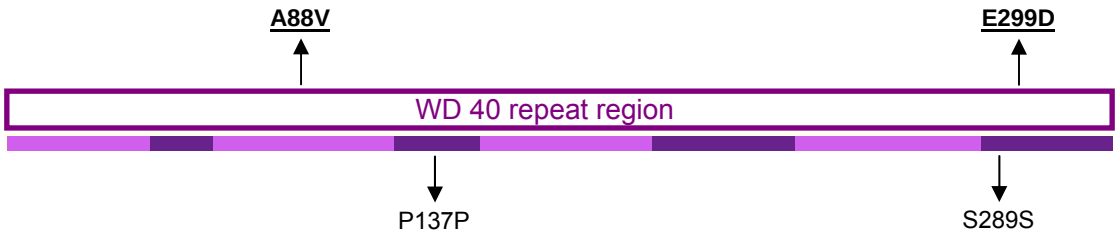

Figure 4.6 Coding *GβL* variants in the SIR cohort
Schematic of the GβL protein showing exons in alternating bright and dark purple and features of the peptide sequence in boxes. Arrows indicate the location of coding SNPs detected in *GβL* by sequencing 158 patients with syndromes of severe insulin resistance. Non-synonymous variants absent from controls (underlined) were considered potentially pathogenic.

```
H. sapiens          PIISYDGVNKNIASVGFHEDGRWMYTGGED   WCVETGEIKREYGGHQK
P. troglodytes      PIISYDGVNKNIASVGFHEDGRWMYTGGED   WCVETGEIKREYGGHQK
M. musculus         PIISYDGVSKNIASVGFHEDGRWMYTGGED   WCVETGEIKREYGGHQK
R. norvegicus       PIISYDGVSKNIASVGFHEDGRWMYTGGED   WCVETGEIKREYGGHQK
G. gallus           PVINYDGVSKNITSVGFHEDGRWMYTGGED   WCVETGEIKREYSGHQK
M. domestica        PVINYDGVSKNITSVGFHEDGRWMYTGGED   WCVDTGEIKREYGGHQK
D. rerio            PVINYDGVSKNITSVGFHEDGRWMYTGGED   WCVETGEIKREYSGHQK
D. melanogaster     PVINFDGVQKNVTRLGFQEDGNWMFTAGED   WKLQTKSSIRDYTGHTK
S. cerevisiae       PVASFEGHRGNVTSVSFQQDNRWMVTSSED   WDLSTREIVRQYGGHHK
```

Figure 4.7 Multiple sequence alignments (using ClustalW) around *GβL* amino acids A88 and E299
Straight lines indicate hidden sequence.

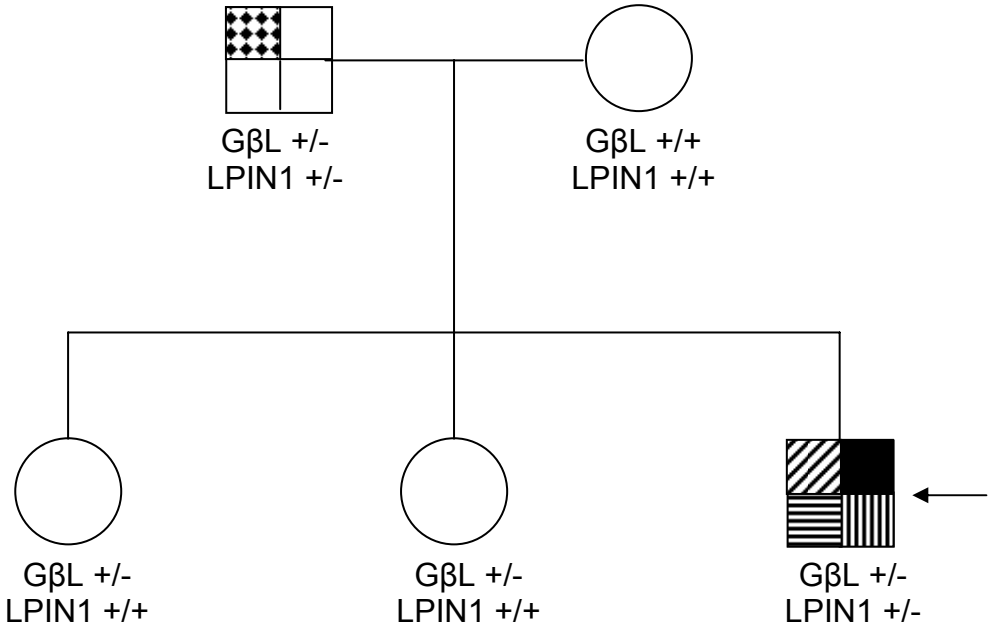

Figure 4.8 A family pedigree demonstrating that the *GβL* A88V and *LPIN1* G582R mutation do not segregate with disease in a fully penetrant manner
+/- represents a heterozygous genotype and +/+ represents the wild-type genotype. The patient (indicated by the arrow) has hyperinsulinaemia (diagonal stripes), severe peripheral neuropathy (black), previous bone marrow transplant for AML (horizontal stripes) and an intracerebral cavernous haemangioma (vertical stripes). His father has diabetes (diamonds).

4.3.3.2 Investigation of the E299D variation

E299D was detected in a female Asian patient with insulin resistant diabetes mellitus. It was also absent from the CIN control panel, which includes 47 Indian DNA samples and 47 European samples. No family were available for co-segregation analysis. Alignment of multiple *GβL* orthologs shows that E299 is not well conserved through evolution as although E is present in chimpanzee, mouse, rat, chicken and zebrafish, in opossum the corresponding residue is D (Figure 4.7). This, and the outcome of SIFT, PolyPhen, and PANTHER prediction programs (data not shown), suggest that this variant does not have a major deleterious impact on the protein and I decided not to follow this further.

4.3.4 *MAPKAP1* sequencing in the SIR cohort

A total of 37 *MAPKAP1* variants were detected in insulin resistant patients (Table A12), five of which were present in the coding sequence (Table 4.4 and Figure 4.9). Synonymous changes were considered unlikely to be pathogenic (shown below the schematic in Figure 4.9). There was one non-synonymous substitution, S260N, that reconfirmed in patient genomic DNA and was absent from 11 Asian and 23 CEPH controls.

4.3.4.1 Investigation of the S260N variation

S260N was present in two female patients, one white European with hyperandrogenism and acanthosis nigricans, and one of mixed ethnicity with pseudoacromegaly. Given that it was present in two of 158 patients I decided to sequence 96 regional controls. The variant was present in one Ely participant with fasting insulin of 42.1 pmol/l, fasting glucose of 5.2 mmol/l, and a BMI of 23.96. It is therefore likely that this variant is a rare, neutral polymorphism.

Table 4.4 *MAPKAP1* coding sequence variants detected in a cohort of severe insulin resistant patients and 11 Indian and 23 CEPH controls

Genic position	Genomic position	Minor|Major allele	Protein consequence	MAF in SIR	Detected in controls?	rs ID
Exon 5	127387762	T|C	D188D	0.005		
Exon 5	127387705	T|C	I207I	0.005		
Exon 6	**127361802**	**T|C**	**S260N**	**0.0161**	**No**	
Exon 7	127345211	T|C	K302K	0.0069		rs11542134
Exon 8	127286607	A|G	H345H	0.2173		rs2070113

Genomic coordinates correspond to NCBI Build 36.

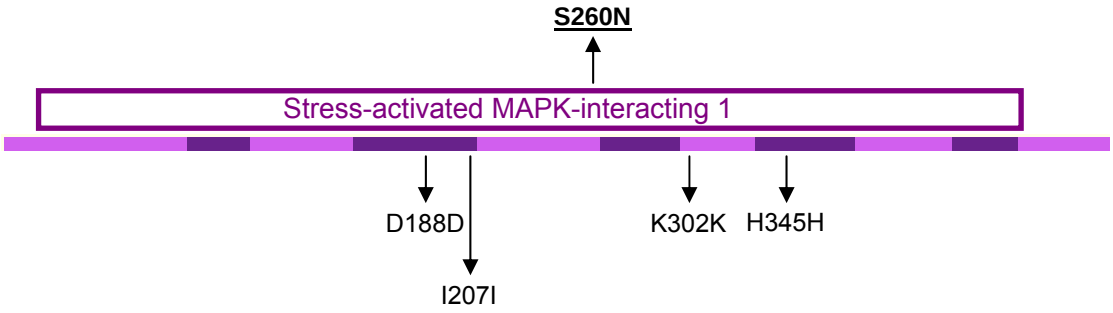

Figure 4.9 Coding *MAPKAP1* variants in the SIR cohort
Schematic of the MAPKAP1 protein showing exons in alternating bright and dark purple and the region conserved between members of the SIN1 family of proteins in boxes. Arrows indicate the location of coding SNPs detected in *MAPKAP1* by sequencing 158 patients with syndromes of severe insulin resistance. Non-synonymous variants absent from controls (underlined) were considered potentially pathogenic.

4.3.5 *AS160* sequencing in the SIR cohort

Sequencing of *AS160* was carried out in collaboration with Satya Dash at the Institute of Metabolic Science, University of Cambridge. Satya Dash sequenced a subset of the severe insulin resistance cohort with high post-prandial to fasting insulin ratios and found a point mutation in exon 3 that leads to replacement of an arginine residue with a premature stop codon at position 363.

I sequenced *AS160* exons and exon-intron boundaries in the entire SIR cohort and detected 28 variants (Appendix Table A13), 11 of which were located in coding regions (Table 4.5 and Figure 4.10). In addition to the R363X mutation I also identified eight non-synonymous changes, three of which were absent from controls (underlined above the schematic in Figure 4.10). The R363X was investigated further by Satya Dash and colleagues. I investigated the remaining three variants at the Wellcome Trust Sanger Institute.

Table 4.5 *AS160* coding sequence variants detected in a cohort of severe insulin resistant patients and 11 Indian and 23 CEPH controls

Genic position	Genomic position	Minor|Major allele	Protein consequence	MAF in SIR	Detected in controls?	rs ID
Exon 1	74953821	G|C	P28P	0.255		rs7327548
Exon 1	74953603	T|C	A101V	0.075	Yes	
Exon 2	**74834347**	**A|G**	**R299Q**	**0.0104**	**No**	
Exon 3	**74831989**	**T|C**	**R363X**	**0.0053**	**No**	
Exon 10	**74798404**	**T|A**	**N655Y**	**0.0052**	**No**	
Exon 13	74785004	G|A	T752A	0.0053	Yes	
Exon 13	**74784903**	**G|C**	**N785K**	**0.0106**	**No**	
Exon 14	74782217	G|A	V819I	0.14	Yes	rs1062087
Exon 16	74778517	A|G	K895K	0.005		
Exon 16	74774390	C|T	L967L	0.3333		rs2297208
Exon 19	74764285	T|C	T1147M	0.1	Yes	rs9600455

Genomic coordinates correspond to NCBI Build 36.

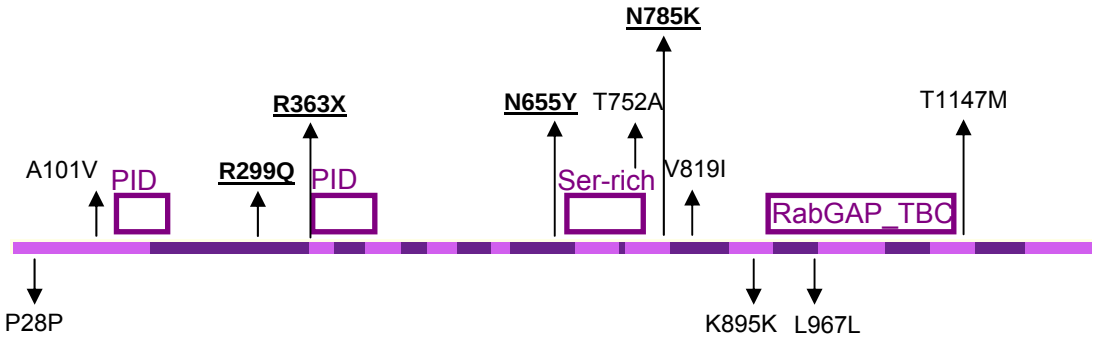

Figure 4.10 Coding *AS160* variants in the SIR cohort
Schematic of the AS160 protein showing exons in alternating bright and dark purple and known functional domains in boxes. Arrows indicate the location of coding SNPs detected in *AS160* by sequencing 158 patients with syndromes of severe insulin resistance. Non-synonymous variants absent from controls (underlined) were considered potentially pathogenic. PID (amino acids 130-188 and 366-438) = phosphotyrosine interaction domain and RabGAP_TBC (amino acids 915-1134) = Rab GTPase activator protein domain.

4.3.5.1 Investigation of the R363X variation

4.3.5.1.1 The patient

R363X was present in a female patient who, at age 11 years, presented with acanthosis nigricans and a BMI standard deviation score (SDS) +2.7. Her fasting glucose and insulin levels fell within age-/gender- and BMI-matched ranges but, following an oral glucose challenge, she displayed dramatic hyperinsulinaemia, with a peak to fasting insulin ratio of 62. By age 23 years her BMI standard deviation score had dropped to SDS 1.4 and her acanthosis nigricans resolved. Although her glucose tolerance had now normalized, she maintained an elevated peak to fasting insulin ratio of 14.

4.3.5.1.2 Family co-segregation analysis

The patient's half-sister presented with acanthosis nigricans and BMI SDS +3.5 at age 9 years and was shown to carry R363X. The mutation was also present in the patient's mother and maternal aunt, both of whom had no acanthosis nigricans but did display elevated peak to fasting insulin ratios at the time of testing (15 and 17

respectively), and the patient's maternal grandmother who was obese and had an elevated fasting glucose (118.9 mg/dL), rendering her peak to fasting insulin ratios uninterpretable. Another maternal aunt had normal glucose tolerance, a peak to fasting insulin ratio of 7, and did not carry R363X (Figure 4.11). Therefore, this mutation appears to segregate with elevated peak to fasting insulin ratios in the family.

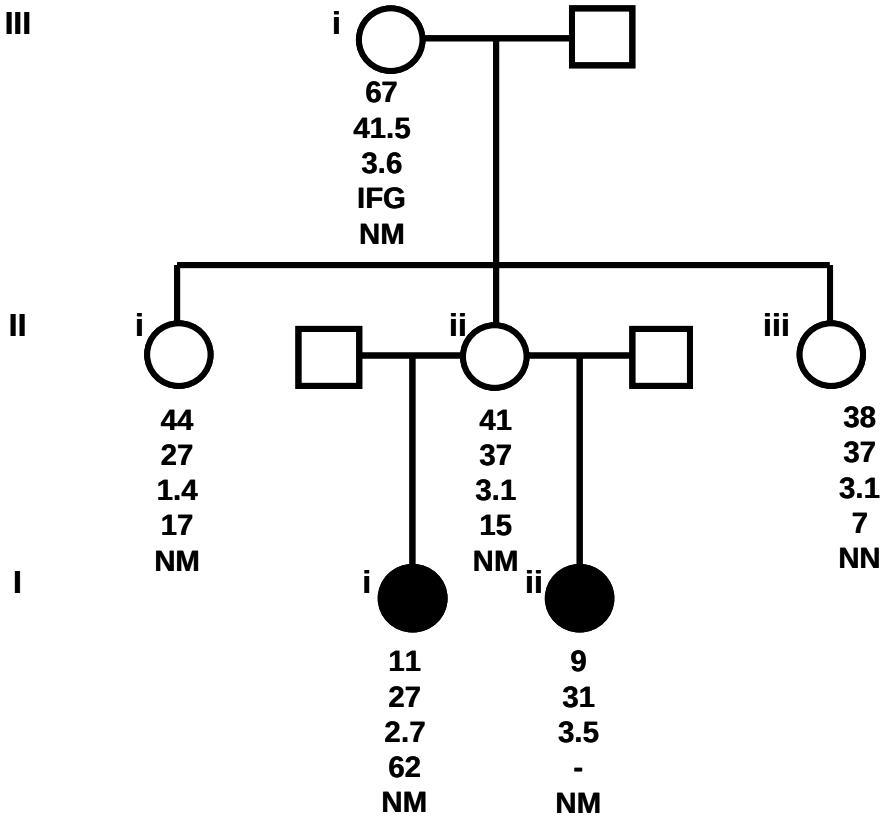

Figure 4.11 Pedigree demonstrating segregation of the *AS160* R363X variation with elevated fasting-to-peak insulin levels in the family of an insulin resistant patient (Ii), taken from (Dash et al., manuscript submitted). Black circles represent females with acanthosis nigricans. Underneath the symbols are shown age at measurement, BMI (kg/m^2), the BMI standard-deviation score (SDS), peak-to-fasting insulin ratios, and genotype (N = R363 and M = X363). IFG = impaired fasting glucose.

4.3.5.1.3 Functional analysis of R363X

Constructs carrying wild-type AS160, AS160 with substitution of a stop codon for an arginine codon (R363X), or a truncated version of AS160 which is missing the sequence from residue 363 (363Tr), were transfected by Satya Dash into 3T3L1

adipocytes. R363X and 363Tr constructs increased cell surface GLUT4 in the basal state and significantly inhibited insulin-stimulated GLUT4 translocation to the plasma membrane (Figure 4.12) compared to wild-type. Truncated protein and wild-type AS160 both bind to full length AS160 *in vitro* (Figure 4.13).

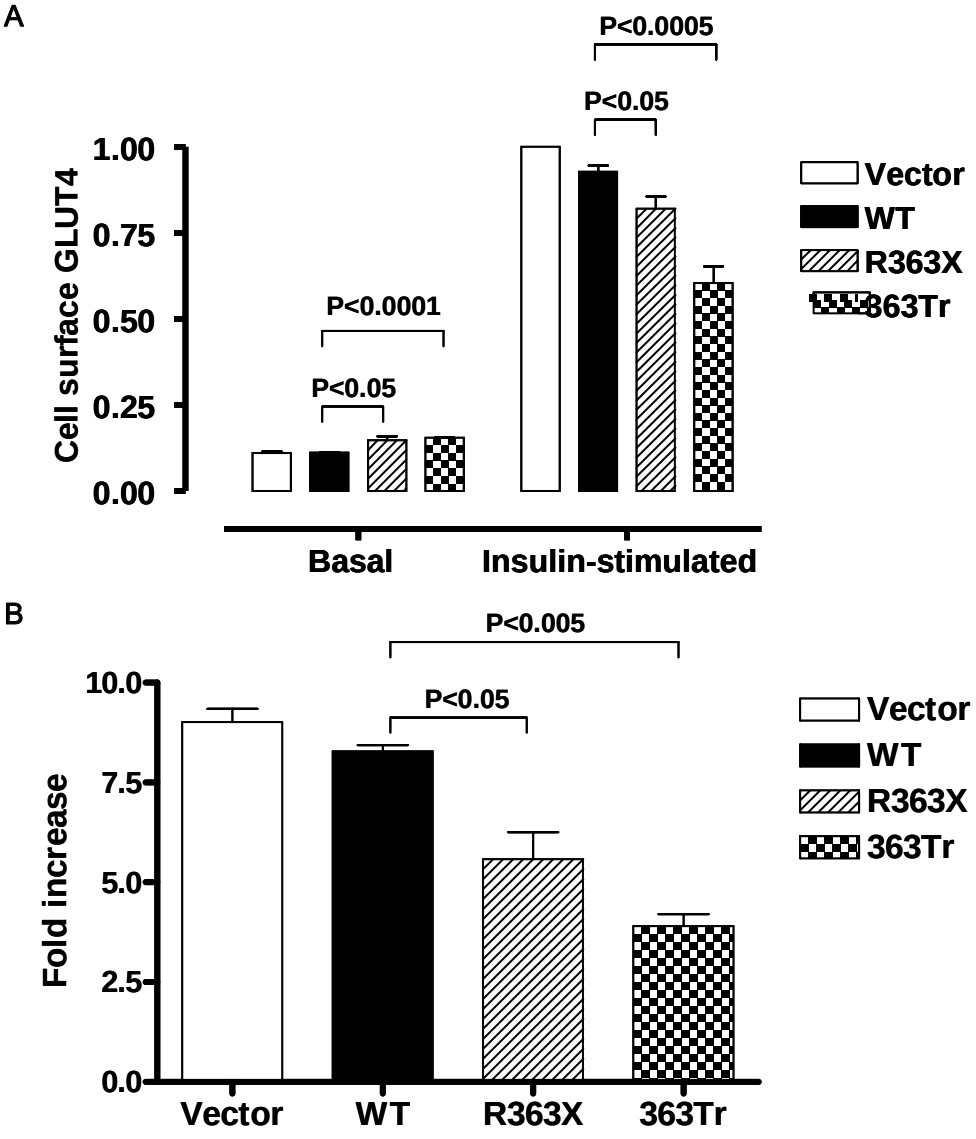

Figure 4.12 Differences in insulin-stimulated GLUT4 expression in cells carrying mutant vs wild-type *AS160*, taken from (Dash et al., manuscript submitted). **A)** Cell surface GLUT4 level, normalized to a value of 1.0 for the vector control in the insulin-stimulated state. Values are expressed as means ± SEs for 4-6 independent measurements of the Cy3/ GFP ratio in cells with and without 30 minutes treatment with 160 nM insulin and **B)** Data expressed as the ratio of cell surface GLUT4 in the insulin-stimulated state to that in the basal state. The R363X construct carries the R363X substitution, whereas the 363Tr carries the gene sequence up to residue 363.

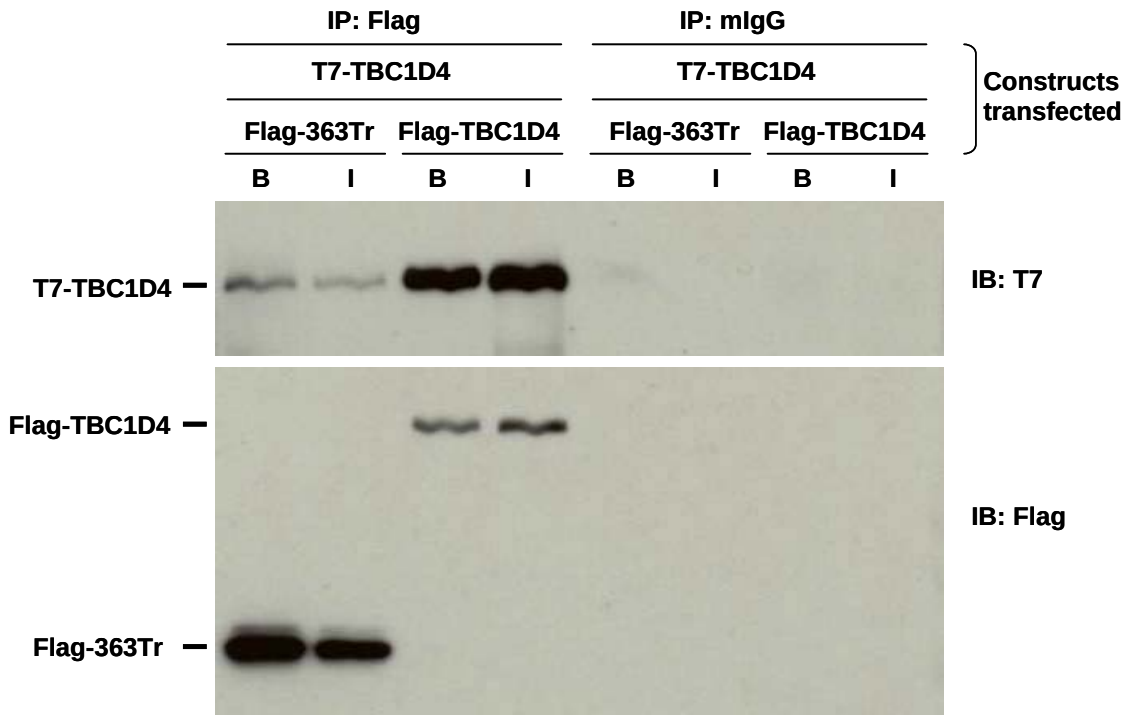

Figure 4.13 Immunoblots (IB) showing co-immunoprecipitation of T7-tagged AS160 (TBC1D4) from basal (B) and insulin-stimulated (I) 293 cells with Flag-tagged truncated AS160 (363Tr) or full-length AS160 (TBC1D4), taken from (Dash et al., manuscript submitted). To control for non-specific immunoprecipitation, lysates were also immunoblotted after immunoprecipitation with irrelevant mouse immunoglobulin and protein G-agarose (mIgG).

4.3.5.2 Investigation of the R299Q variation

R299Q is present in homozygous form in an Arabic female with pseudoacromegaly and acanthosis nigricans and is absent from 164 Arabic controls included in the HGDP panel. There was no family available for co-segregation analysis. Arginine is well conserved in a range of organisms, including chimpanzee, mouse, chicken, opossum, and frog (Figure 4.14) but a change to glutamine at residue 299 is predicted benign by SIFT, PolyPhen and PANTHER. As far as is known the patient is not the offspring of consanguineous union, therefore I would have expected to detect some heterozygotes. It is possible that the patient only appears homozygous because of a deletion in the other copy of the gene. Alternatively, the mutant copy of the gene may be preferentially amplified during PCR and sequencing. This will need to be investigated in future work.

4.3.5.3 Investigation of the N655Y variation

N655Y was detected in an obese, teenaged, white European female with acanthosis nigricans. The variant was present in the proband's obese mother (who is not insulin resistant), and was absent in her unaffected brother (Figure 4.15). Interestingly, a variant in β-melanocyte-stimulating hormone (*β-MSH*) has already been found to segregate with obesity in this family (Lee et al. 2006). It is possible that obesity-induced insulin resistance in the patient is exacerbated by the *AS160* N655Y mutation, though *β-MSH* and *AS160* together do not segregate with insulin resistance in the family. Furthermore, asparagine is not very well conserved at position 655 and there is a tyrosine residue at this position in rat (Figure 4.14), implying that this variant does not have a major deleterious effect.

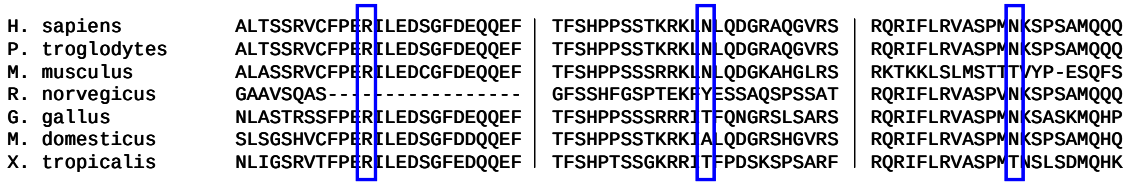

Figure 4.14 Multiple sequence alignments (using ClustalW) around *AS160* amino acids R299, N655 and N785
Straight lines indicate hidden sequence.

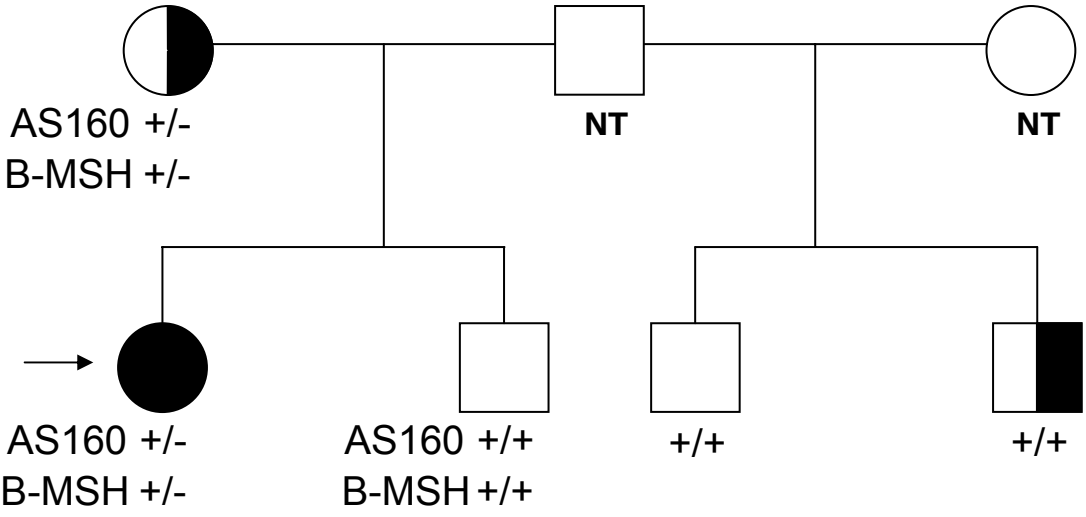

Figure 4.15 Presence of *AS160* N655Y and a previously reported *β-MSH* mutation in a family of a patient with obesity and insulin resistance
+/- represents a heterozygous genotype and +/+ represents the wild-type genotype. The patient (indicated by the arrow) is obese and insulin resistant. The mother and half brother with black and white symbols are also obese.

4.3.5.4 Investigation of the N785K variation

N785K was detected in an Asian male patient with early-onset diabetes and acanthosis nigricans, and by Satya Dash in an Asian female patient with hyperandrogenism, insulin resistance and acanthosis nigricans. Its presence in two Asian patients suggested that this variant might be an uncommon Asian polymorphism and indeed Satya Dash detected N785K in one of 95 Punjabi controls. In mouse and frog the asparagine is replaced by a threonine residue (Figure 4.14), and SIFT, PolyPhen, and PANTHER program predict that the change to lysine has no functional effect on the protein.

4.3.5.5 Summary of *AS160* mutation screening

In summary, four rare *AS160* variants that alter the protein sequence were detected in the SIR cohort, one of which lead to a premature stop codon early in the peptide sequence (R363X). R363X was extensively investigated by Satya Dash and his colleagues at the University of Cambridge. Three amino acid substitutions were also detected, none of which fell within known functional domains. R299Q is present in a patient with pseudoacromegaly and acanthosis nigricans but absence of DNA from family members prevented further analysis. N655Y was detected in an obese insulin resistant patient, in whose family obesity was likely caused by a *β-MSH* mutation. N785K was detected in two insulin-resistant Asian patients and a Punjabi control so this variant is likely to be a rare Asian polymorphism and was not investigated further.

4.3.6 *Raptor* sequencing in the SIR cohort

A total of 190 *Raptor* variants were detected in insulin resistant patients (Appendix Table A14), 29 of which were present in the coding sequence (Table 4.6 and Figure 4.16). None of the three non-synonymous variants were present in controls (underlined above the schematic in Figure 4.16). Due to time constraints, *Raptor* variants were prioritised for further study based on evolutionary conservation (Figure 4.17) and the predictions of bioformatics programs. G187S and A862T were predicted benign by PolyPhen and PANTHER and are not very well conserved (Figure 4.17). R997H is predicted to have a possible functional effect and is well conserved in vertebrates. For this reason R997H was investigated further.

4.3.6.1 Investigation of the R997H variation

R997H was detected in an Asian female with hyperandrogenism, insulin resistance, and acanthosis nigricans. The variant was also found in one CIN control and was therefore considered unlikely to be pathogenic.

Table 4.6 *Raptor* coding sequence variants detected in a cohort of severe insulin resistant patients and 11 Indian and 23 CEPH controls

Genic position	Genomic position	Minor|Major allele	Protein consequence	MAF in SIR	Detected in controls?	rs ID
Exon 1	76134114	C|T	F30F	0.0967		
Exon 2	76214157	G|C	T78T	0.2005		rs17848685
Exon 5	76319006	A|G	G187S	0.0026	No	
Exon 5	76319008	G|C	G187G	0.0053		
Exon 6	76342542	G|C	T264T	0.0026		
Exon 11	76434924	C|T	G423G	0.3617		rs3751945
Exon 11	76434969	A|G	Q438Q	0.1058		rs2589156
Exon 14	76468818	G|A	Q506Q	0.2526		rs2289759
Exon 15	76471873	A|G	T548T	0.0053		rs34848699
Exon 16	76472295	A|G	S590S	0.0058		
Exon 17	76473438	T|C	F626F	0.0028		
Exon 17	76473495	T|C	A645A	0.0028		
Exon 18	76480141	C|T	L670L	0.2526		rs2289764
Exon 18	76480225	G|A	A698A	0.1349		rs2289765
Exon 22	76511124	T|C	T842T	0.2919		rs2271603
Exon 22	76511182	A|G	A862T	0.0036	No	
Exon 24	76513818	A|G	T954T	0.0028		
Exon 25	76528905	T|C	H978H	0.0054		
Exon 25	76528961	A|G	R997H	0.0031	No	
Exon 26	76534153	T|C	A1039A	0.3521		rs1567962
Exon 28	76537938	A|G	T1122T	0.0026		
Exon 30	76548509	T|C	L1172L	0.0029		
Exon 31	76549792	T|C	R1203R	0.3411		rs9899178
Exon 31	76549870	C|T	S1229S	0.0088		

Genomic coordinates correspond to NCBI Build 36.

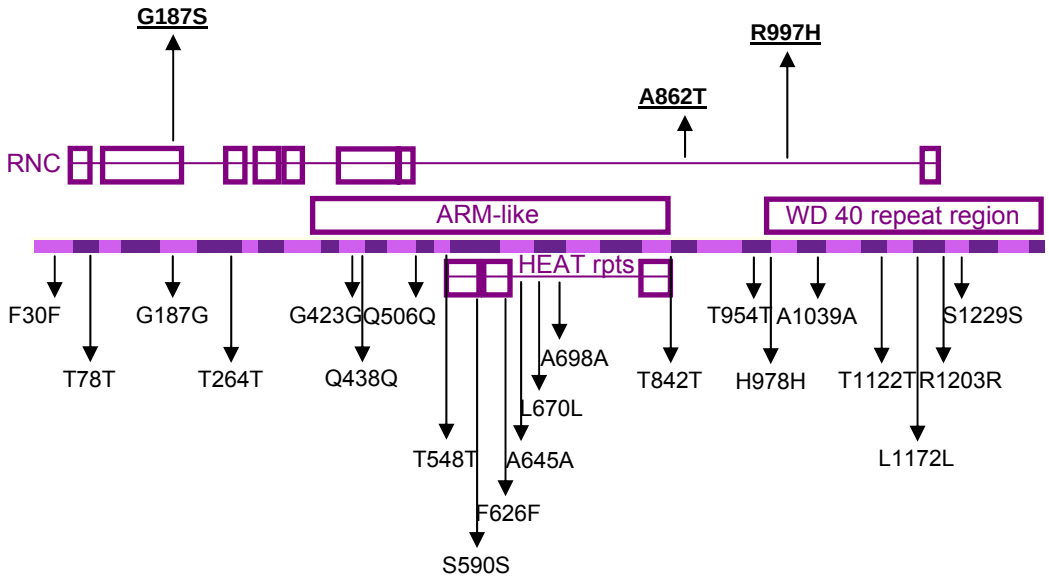

Figure 4.16 Coding *Raptor* variants in the SIR cohort
Schematic of the Raptor protein showing exons in alternating bright and dark purple and known functional domains in boxes. Arrows indicate the location of coding SNPs detected in *Raptor* by sequencing 158 patients with syndromes of severe insulin resistance. Non-synonymous variants absent from controls (underlined) were considered potentially pathogenic. RNC (amino acids 53-1196) = raptor N-terminal conserved domain and ARM-like (amino acids 372-839) = Armadillo repeat.

```
H. sapiens          QTWMGSPSIFVY | TQSAPASPTNKG | FLRNSRVRRQAQ
P. troglodytes      QTWMGSPSIFVY | TQSAPASPTNKG | FLRNSRVRRQAQ
M. musculus         QTWMGSPSIFVY | TQSAPASPTNKG | FLRNTRVRKQAQ
R. norvegicus       QTWMGSPSIFVY | TQSAPASPTNKG | FLRNTRVRKQAQ
G. gallus           QTWMGSPSIFVY | TQSAPASPTNKG | FLRNARVRKQAQ
M. domesticus       QTWMGSPSIFVY | TQSAPASPTNKG | FLRNTRVRKQAQ
X. tropicalis       QTWMGSPSIFVY | TQSAPASPTNKG | FLRNTRVRKQAQ
D. melanogaster     ITWMSAPSIYVY | AESPPVGAAASG | FLRNDFVRRHAG
S. cerevisiae       QTWLGAPCIFVY | SFSPMERVDNNA | RNRNETIIQETQ
```

Figure 4.17 Multiple sequence alignments (using ClustalW) around *Raptor* amino acids G187, A862, and R997
Straight lines indicate hidden sequence.

4.4 Discussion

mTOR complexes are important components of the insulin signalling pathway. mTORC1 modulates insulin sensitivity in response to growth factors, hormones, nutrients, energy status, and cellular stressors, while mTORC2 phosphorylates a critical kinase, AKT, required for insulin-stimulated glucose uptake. I have sequenced 158 patients with syndromes of severe insulin resistance for genes encoding components of mTORC1 and mTORC2, including *mTOR*, *GβL*, *Rictor*, *Raptor*, *MAPKAP1*, as well as a Rab-GAP protein (*AS160*), which is the substrate of AKT proteins and regulates GLUT4 trafficking to the cell surface. Eleven rare non-synonymous variants and a putative truncating mutation absent from a total of 59 controls were detected across these genes. A combination of analyses including family cosegregation analyses, sequencing of ethnically-matched controls, and prediction of functional effects based on evolutionary conservation indicated that the rare nonsynonymous variants in *mTOR*, *Rictor*, *Raptor*, *GBL*, *MAPKAP1* and *AS160* were not likely to be fully pathogenic in patients with severe insulin resistance. The stop mutation in *AS160* (R363X) segregated with high peak-to-fasting insulin ratios in a family with five affected members. *In vitro* studies demonstrated that this mutation impairs insulin-stimulated GLUT4 translocation to the plasma membrane and could disrupt activity of wild-type AS160.

The *AS160* variant R363X resulted in a premature stop codon after the first phosphotyrosine interaction domain (PID) but before the second PID and the Rab-GAP domain. This would be expected to disrupt the ability of the protein to hydrolyse Rab-GTP to Rab-GDP. Furthermore, all predicted AKT phosphorylation sites will be absent from the truncated AS160 protein potentially preventing its regulation of GLUT4 trafficking in response to insulin. Satya Dash at the Institute of Metabolic Science (IMS) in Cambridge demonstrated that the R363X co-segregated with higher

than average peak-to-fasting insulin levels in the family (Satya et al., unpublished). This phenotype seems consistent with the role of AS160 in insulin-stimulated GLUT4 trafficking. Disruption of the cell's ability to translocate GLUT4 to the membrane to facilitate glucose uptake would result in slower post-prandial glucose clearance and higher compensatory peak insulin levels, but might not be expected to affect basal insulin levels. Functional analyses undertaken at the IMS showed that the truncated protein significantly reduced insulin-stimulated GLUT4 translocation to the cell surface *in vitro*.

The proband and relevant family members are heterozygous for R363X, so this variant could be causing insulin resistance through haploinsufficiency or a dominant negative effect. In vitro studies demonstrated that AS160 exists as a dimer (unpublished observations of Cristinel Miinea and G.E.L., and Figure 4.12) and that truncated AS160 can bind the full length protein. This suggests that the mutation can act as a dominant negative mutation.

Given that the remaining eleven variants in mTORC/*AS160* genes are less likely to cause disease in a fully penetrant manner it would appear that point mutations and small insertion /deletions in components of mTORCs are not common causes of human severe insulin resistance. However, for several of these variants it was impossible to perform co-segregation analyses as DNA from family members of the patient was not available. It is difficult to establish pathogenicity in the absence of family members and, especially in smaller pedigrees, a variant can appear to segregate with disease by chance. Investigation of the candidate gene or variant in other similarly affected individuals and families might help build support for its involvement in disease. The same genetic factor might segregate with disease in multiple affected families, or affected individuals may be enriched for different rare functional variants in the same gene compared to controls. These studies would require large sample sizes of well-phenotyped cases of disease and control

individuals. Alternatively, a disease-causing variant may be unique to a particular individual/family (or in other words, the disease may be unique) rendering larger study sizes useless for establishing stronger evidence for pathogenicity. In these cases, functional studies may be the only way to establish whether and how a variant affects protein function and causes disease. As functional assays can be time-consuming to design and optimise, it is difficult to test every putative pathogenic mutation for a functional effect. Bioinformatics programs such as SIFT, PolyPhen, and PANTHER have been designed to assess the likelihood that an amino acid change is deleterious to protein function based on evolutionary conservation and the biochemistry of the residues involved. However, these programs should not be used as proof of a functional effect or lack thereof, and cannot explain how a functional variant may be impacting disease. These issues surrounding the investigation of Mendelian diseases will also be relevant to whole-genome resequencing studies, made possible by faster and cheaper sequencing technology (Ng et al. 2008b). My screening studies suggest that resequencing of all known exons in the genome will uncover many putative disease mutations. However, in the absence of large pedigrees and appropriate functional assays it may be difficult to determine the true functional variants behind Mendelian phenotypes.

As I only screened 158 patients with syndromes of severe insulin resistance, I cannot rule out variation in mTORC components as rarer causes of severe insulin resistant syndromes. Furthermore, I did not screen patients for mutations in promoter/enhancer/regulatory regions that may impact expression levels, or for large copy number changes such as deletions of whole exons. These changes cannot therefore be excluded as causes of severe insulin resistance in the cohort.

In conclusion, my screening efforts in components of mTOR complexes and *AS160* lead to the discovery of a stop mutation in *AS160* that impairs insulin-stimulated

GLUT4 translocation and segregates with high peak-to-fasting insulin levels in a family with five affected individuals. I recommend screening *AS160* in families with similar phenotypes for additional mutations, which would help corroborate these findings. Other putative functional variants were considered unlikely to be fully pathogenic but demonstrate that, in the absence of family members for co-segregation analyses and validated functional assays, it is difficult to establish the impact of rare genetic factors on Mendelian disease. These are issues that will affect future studies of Mendelian traits in the era of whole-genome sequencing.

4.5 Materials and Methods

4.5.1 Description of cohorts

See Chapter 2 for details of the cohorts. Briefly, the severe insulin resistance cohort comprises 158 patients with syndromes of severe insulin resistance, and the control cohorts comprise unaffected individuals of Northern and Western Europe (CEPH N=48), European-Indian (CIN panel N=94), and 164 individuls of Arabic ancestry (HGDP).

4.5.2 PCR and sequencing

Genomic DNA from 158 patients with syndromes of severe insulin resistance, 11 Indian controls (from the CIN panel, Appendix Table A4) and 23 CEPH controls was whole-genome amplified (Chapter 2.3.1.1). Primers were designed to amplify *mTOR*, *Rictor*, *GBL*, *MAPKAP1*, *AS160*, and *Raptor* exons, exon-intron boundaries and 3'UTR (see Appendix Table A15 for sequences and conditions). PCR and product purification were performed using the standard procedure outlined in Chapter 2.3.2. Bi-directional sequencing was performed with M13 primers using the Big Dye Terminator 3.1 kit (Applied Biosystems, Foster City, CA, USA) (see Chapter 2 for details). Sequencing reactions were run on ABI3730 capillary machines (Applied Biosystems) and analysed using Mutation Surveyor version.2.20 (SoftGenetics LLC, State College, PA, USA) or GAP4 (Staden Sequence Analysis Package software). All non-synonymous variants with MAF<0.01 were confirmed in a second PCR and sequencing reaction using patient genomic DNA. Three web-based programs were employed to predict the likelihood that point mutations had a functional impact on the protein (Chapter 2.3.6). DNA from family members used for co-segregation analysis was genomic.

4.5.3 In vitro studies of mutant AS160 function

Satya Dash and colleagues at the Institute of Metabolic Science, University of Cambridge, first identified and investigated the functional consequences of the R363X mutation in *AS160*. Human wild type *AS160* in the P3XFLAG CMV10 vector (Kane et al. 2002) was used to generate a Flag-tagged mutant construct using the QuikChangeTM site directed mutagenesis kit (Stratagene) according to the manufacturer's protocols. In order to evaluate the biological effects of the truncated mutant, a second construct was created in this vector with no coding DNA beyond the stop codon identified in the proband (designated 363Tr) (Dash et al., manuscript submitted).

The relative amount of GLUT4 at the cell surface in 3T3-L1 adipocytes was assayed by transfecting cells through electroporation with a plasmid for expression of HA-GLUT4-GFP and measuring the HA-GLUT4-GFP at the cell surface by quantitative single-cell immunofluorescence, as previously described (Sano et al. 2003). In this method, HA-GLUT4-GFP at the cell surface is labelled with anti-HA and Cy3-conjugated secondary antibody; the fluorescence intensities for Cy3 and GFP in individual cells are quantitated; and the relative amount of HA-GLUT4-GFP at the cell surface is expressed as the ratio of Cy3 to GFP, in order to correct for different levels of expression of the HA-GLUT4-GFP protein.

The association of AS160 with itself and with the 363Tr form was examined by co-transfecting human embryonic kidney 293E cells with plasmids for expression of N-terminal T7-tagged human AS160 and either N-terminal Flag-tagged AS160 or the 363Tr with Lipofectamine 2000. The cells were treated with insulin (1 µM for 10 minutes) or left unstimulated, then lysed in 40 mM Hepes, 150 mM NaCl, pH 7.4 containing 1.5 % nonionic detergent octaethyleneglycol dodecyl ether and protease and phosphatase inhibitors. The lysate was cleared by centrifugation at 12,000 x g for

15 minutes and the portions of the supernatant were immunoprecipitated with anti-Flag agarose or irrelevant mouse immunoglobulin and protein G-agarose. SDS samples of the immunoprecipitates were immunoblotted for the T7 and Flag epitopes.

4.5.4 Statistical Analysis

GLUT4 translocation data are expressed as means ± SE. Differences between vectors were compared with use of the unpaired Student's t-test. All reported P values are from two-sided tests, and P values of less than 0.05 were considered to indicate statistical significance.